THE BELL SYSTEM TECHNICAL JOURNAL
Vol. 50, No. 3, March, 1971
Printed in U.S.A.

Number and Duration of Fades at 6 and 4 GHz

By ARVIDS VIGANTS

(Manuscript received November 9, 1970)

We present in this paper experimental and theoretical results on the number of fades, average durations of fades, and the probability distributions of fade durations for line-of-sight microwave transmission in the 6- and 4-GHz bands. Both fading of single signals and simultaneous fading of pairs of signals within each of the two bands are treated. The experimental results are based on data obtained in 1966 in Ohio. Mathematical description of the number and average duration of fades is based on a theory in which pairs of signals are treated as correlated random variables that are jointly Rayleigh distributed. The durations of deep fades of single signals tend to be lognormally distributed. A probability distribution of the duration of simultaneous fades, which agrees with experimental data, is obtained from the lognormal distribution using a heuristic model.

I. INTRODUCTION

Microwave transmission on line-of-sight radio-relay links is affected by the lower atmosphere. When atmospheric conditions permit multipath propagation, the output from a receiving antenna can be practically zero for seconds at a time. Such deep fades are rare events. Still, they are sufficiently numerous to cause problems in high-performance communication systems.

There is a certainty to fading that other causes of outages and performance degradation do not possess. For example, catastrophic equipment failure may or may not occur during the projected life of the equipment on a communications link. On the other hand, come summer and fall, one can state with some assurance that fading will occur on certain links in a particular microwave radio-relay system.

The number of fades and the durations of the fades have a direct bearing on system performance. Previous investigations of frequency

diversity at Bell Laboratories[1,2] and reports on extensive British[3] and Japanese[4] experiments dwell mostly on fade-depth distributions. The available information on fade duration distributions is rudimentary.[5–7]

As a part of a current and continuing effort, both experimental and theoretical, to describe the fundamental properties of line-of-sight microwave channels,[2,8,9] we will present results on the number of fades, the average durations of fades, and the probability distributions of fade durations. Both fading of single signals and simultaneous fading of pairs of signals within a frequency band will be treated. Theoretical description of fading being far from complete, we will put major emphasis on experimental data.

Deep fades rarely occur simultaneously at two frequencies when the frequency separation becomes larger than a few tens of MHz. We will show that this experimental result can be described in terms of a model in which the signals at the two frequencies are treated as correlated random variables that are jointly Rayleigh distributed. We will also show that the observed average fade durations follow from this model. The advantage of the Rayleigh model is that it contains only a small number of parameters.

Durations of deep fades tend to be lognormally distributed. When the durations are normalized to their means, the distribution becomes independent of fade depth. We will show that a heuristic model can be used to describe how the durations of simultaneous fades of two signals are related to fade durations of single signals. The model permits transformation of the lognormal distribution into a distribution for the durations of simultaneous fades.

The final section of this work contains a comparison of the effectiveness of frequency-diversity and space-diversity reception. The results summarized in this section may be of particular interest to readers who need numerical values for diversity, reliability, or interference calculations.

II. FORM OF THE EXPERIMENTAL DATA

The results presented here are based on experimental data obtained at West Unity, Ohio.[2] Briefly, the basic data consist of measurements of received power for signals at various frequencies on a 28.5-mile path. The transmitted power for each signal, which was angle modulated, was constant. The center frequencies of the signals in the 6-GHz and 4-GHz bands are listed in Table I. The received power for each signal was sampled five times a second, converted to a decibel scale,

TABLE I—LIST OF FREQUENCIES

Frequencies			
6-GHz Band		4-GHz Band	
i	GHz	i	GHz
1	5.9452	1	3.750
2	6.0045	2	3.770
3	6.0342	3	3.830
4	6.0638	4	3.850
5	6.1231	5	3.910
6	6.1528	6	4.070
		7	4.170

and recorded in digital form for subsequent computer processing (in the absence of fading the recording rate was less than the sampling rate). The data were obtained during a 68-day period in 1966 (July 22 to September 28). The time covered by the data is 5.26×10^6 seconds. We refer to the 5.26×10^6 seconds as the test period.

During computer processing, the received power for each signal was normalized to its value in the absence of fading. The normalized dB values are denoted by 20 log R_i, where the subscript i identifies a frequency in Table I (the data in the two frequency bands will be discussed separately; there should be no confusion about which of the two bands a subscript refers to). As a consequence of the normalization, the voltage envelopes R_i are unity in the absence of fading.

To investigate simultaneous fading of signals at two frequencies, an envelope consisting of the larger of the two envelopes,

$$R_{ij} = \max (R_i , R_j) \tag{1}$$

was constructed in the computer during the processing of the data. Fifteen such envelopes were constructed in each of the two bands. These are listed in Tables II and III. The frequency separations Δf in Table II have been rounded to the nearest multiple of 30 MHz. The parameter q, discussed later, will be used in the description of simultaneous fading.

An idealized picture of fading is shown in Fig. 1. A signal is said to be in a fade of depth 20 log L when its envelope becomes less than L. We refer to fades of R_{ij} as simultaneous fades. We limit our discussion to fades deeper than -20 dB; that is, to values of L that are less than a tenth.

TABLE II—LIST OF FREQUENCY PAIRS IN THE 6-GHz BAND

Δf in MHz	ij	q	Figure
30	23	0.001	6
30	34	0.001	7
30	56	0.001	8
60	12	0.002	9
60	24	0.002	10
60	45	0.002	11
90	13	0.004	12
90	35	0.004	13
90	46	0.004	14
120	14	0.005	15
120	25	0.005	16
120	36	0.005	17
150	26	0.007	18
180	15	0.007	19
210	16	0.010	20

TABLE III—LIST OF FREQUENCY PAIRS IN THE 4-GHz BAND

Δf in MHz	ij	q	Figure
20	12	0.002	21
20	34	0.002	22
60	23	0.007	23
60	45	0.007	24
80	24	0.010	25
80	35	0.010	26
100	14	0.013	27
160	15	0.020	28
160	56	0.020	29
220	46	0.030	30
260	57	0.030	31
300	26	0.035	32
340	37	0.035	33
400	27	0.050	34
420	17	0.050	35

III. NUMBER AND AVERAGE DURATION OF FADES OF SINGLE SIGNALS

The number of fades of depth 20 log L dB is equal to, by definition, the number of times an envelope crosses L in an upward direction (see Fig. 1). The data on this for the six signals in the 6-GHz band and the seven signals in the 4-GHz band are summarized in Figs. 2 and 3 respectively. The data scatter, but the overall impression is that the number of fades is proportional to L. Least-squares fitting of lines

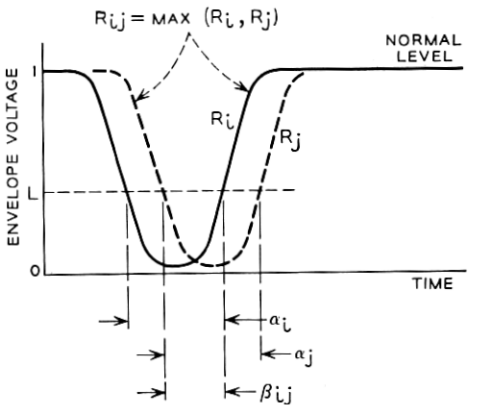

Fig. 1—Definition of terms.

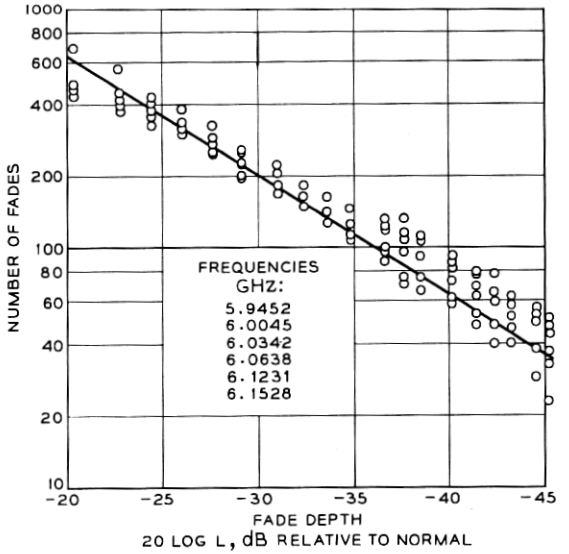

Fig. 2—Summary of the number of fades in the test period of the six single signals in the 6-GHz band (equation of theoretical line is $N = 6410\ L$).

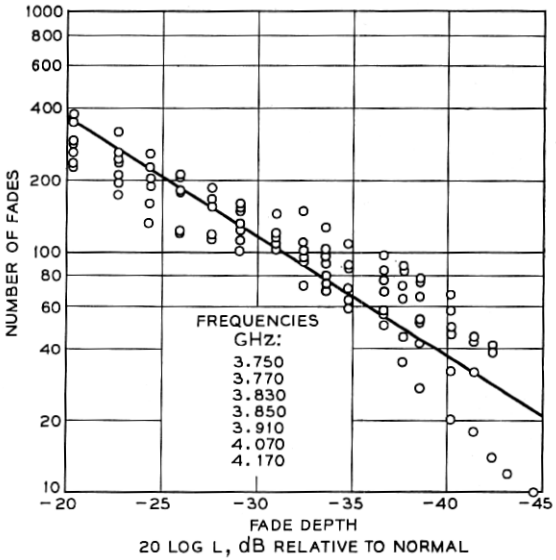

Fig. 3—Summary of the number of fades in the test period of the seven single signals in the 4-GHz band (equation of theoretical line is $N = 3670\ L$).

with this dependence on L to the data gives the following for the number of fades in the test period

$$N = 6410\ L, \text{ in the 6-GHz band,} \tag{2}$$

$$N = 3670\ L, \text{ in the 4-GHz band.} \tag{3}$$

As an example, we note that N in the 6-GHz band averages to roughly one -40 dB fade per day during the test period.

The average durations of fades were obtained by taking the total time spent in fades of a given depth[2] and dividing this by the number of fades of that depth. The resulting data are shown in Fig. 4 for the six signals in the 6-GHz band and in Fig. 5 for the seven signals in the 4-GHz band. The average durations are roughly proportional to L. Least-squares lines with this dependence on L fitted to the data are

$$\langle \alpha \rangle = 490\ L \text{ seconds, in the 6-GHz band,} \tag{4}$$

$$\langle \alpha \rangle = 408\ L \text{ seconds, in the 4-GHz band,} \tag{5}$$

where α denotes fade duration (see Fig. 1), and where the brackets denote averages. The fit of equation (4) to the points in Fig. 4 is better than that of equation (5) to the points in Fig. 5. The points in Fig. 4 are based on a larger number of observations than those in

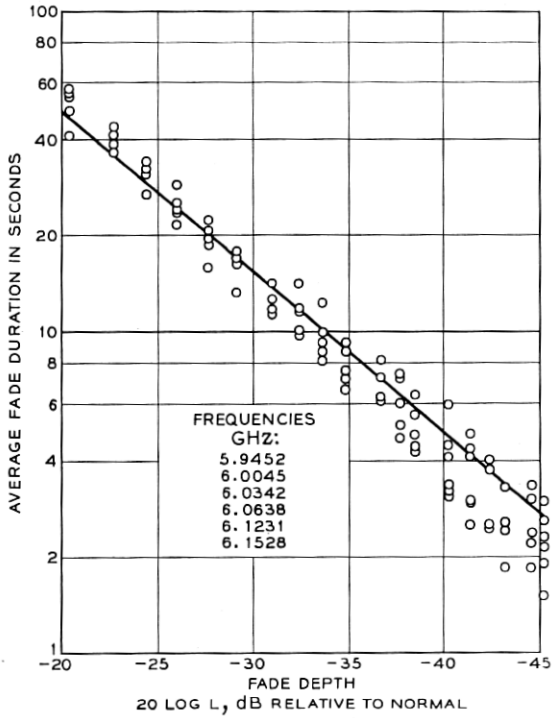

Fig. 4—Summary of the average fade durations of the six single signals in the 6-GHz band (equation of theoretical line is $\langle\alpha\rangle = 490\ L$).

Fig. 5. It is therefore possible that in Fig. 5 we are beginning to see the effects of small sample size. We will assume that this is indeed so and put greater emphasis on the 6-GHz data in the subsequent analysis.

The data show that average fade durations in the −40 dB range are of the order of seconds. This has direct bearing on system performance calculations, where it has been assumed, at times, that deep fades have durations of the order of minutes. (Section 5.2.1 in Ref. 10.)

The total time spent in fades is the product $N\ \langle\alpha\rangle$, which is proportional to L^2. The observed behavior of fade-depth distributions for deep fades is indeed this,[2] which suggests comparison of the experimental results to theoretical results for Rayleigh distributed variables. The theoretical expressions for the number of fades and the average fade durations are, in the case of deep fades,[9,11]

$$N \approx (rT_oc)\ L,\ L < 0.1\ ; \tag{6}$$

$$\langle\alpha\rangle \approx c^{-1}L,\quad L < 0.1; \tag{7}$$

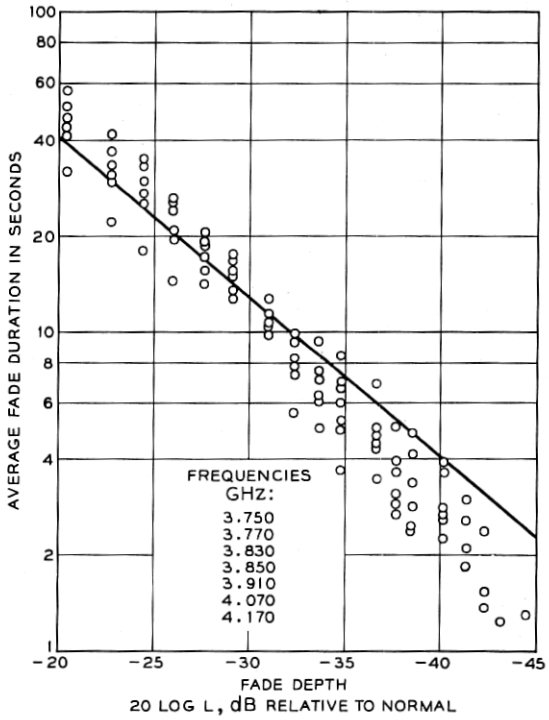

Fig. 5—Summary of the average fade durations of the seven single signals in the 4-GHz band (equation of theoretical line is $\langle \alpha \rangle = 408\ L$).

where the dimensionless factor r is proportional to the amount of time during which atmospheric conditions allow multipath propagation; T_0 is the test period (5.26×10^6 seconds in our case); the quantity c, which has the dimensions of inverse time, is proportional to the spectral width of the fluctuations of R_i. The theoretical equations (6) and (7) clarify the meaning of the coefficients in equations (2) through (5). Numerical values for the parameters r and c can be obtained readily from a comparison of the coefficients. However, r varies with path length and other parameters.[12] We will not discuss this here, because the variability of fading from path to path is a topic in itself.

IV. NUMBER OF SIMULTANEOUS FADES

Simultaneous fades are fades of R_{ij} (see Fig. 1). The experimental results on the number of simultaneous fades are shown in Figs. 6 to 20

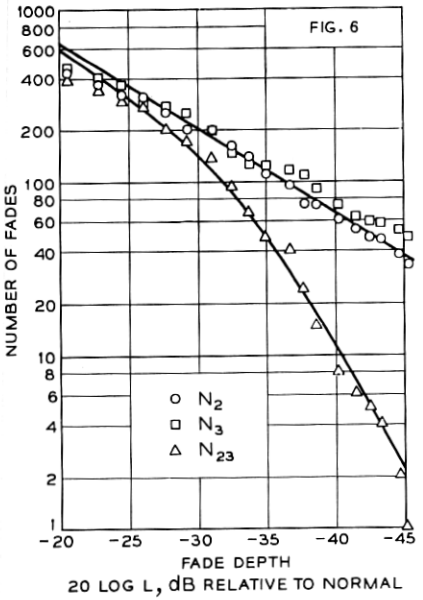

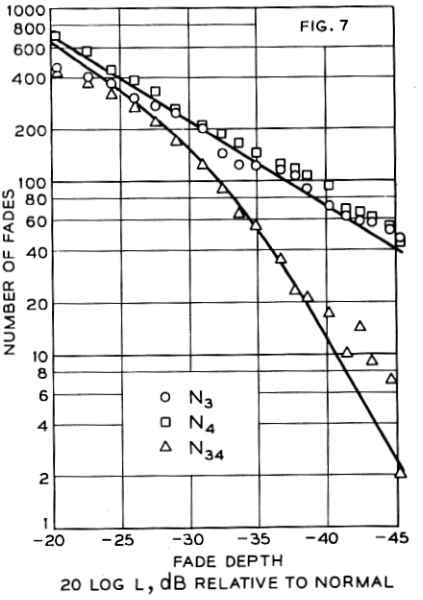

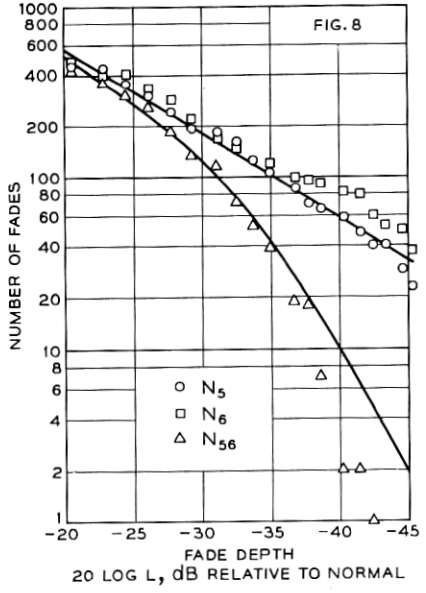

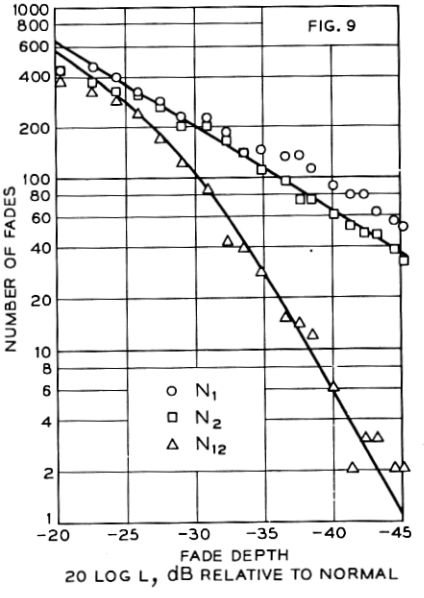

Fig. 6—Number of fades in test period (6-GHz band, $\Delta f = 30$ MHz).
Fig. 7—Number of fades in test period (6-GHz band, $\Delta f = 30$ MHz).
Fig. 8—Number of fades in test period (6-GHz band, $\Delta f = 30$ MHz).
Fig. 9—Number of fades in test period (6-GHz band, $\Delta f = 60$ MHz).

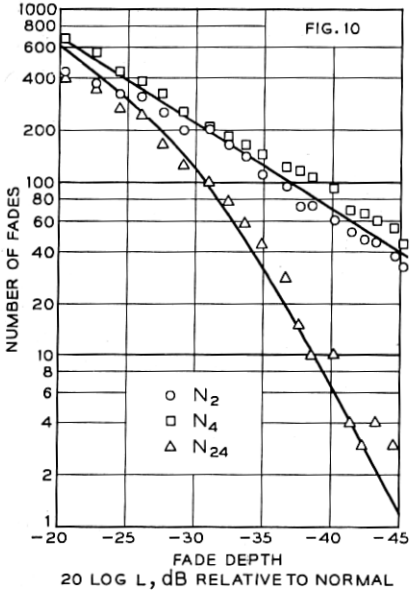

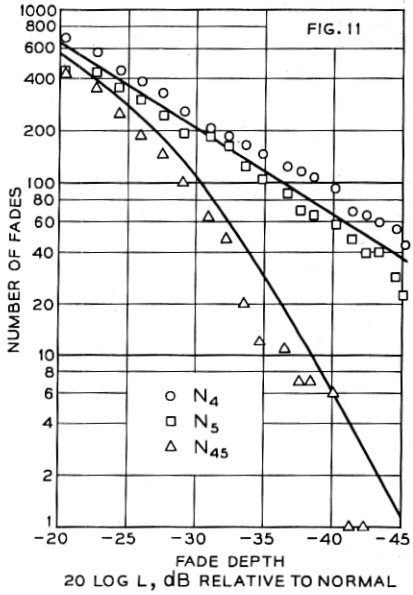

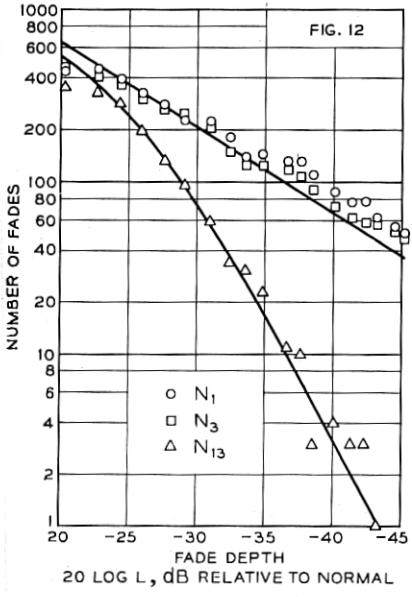

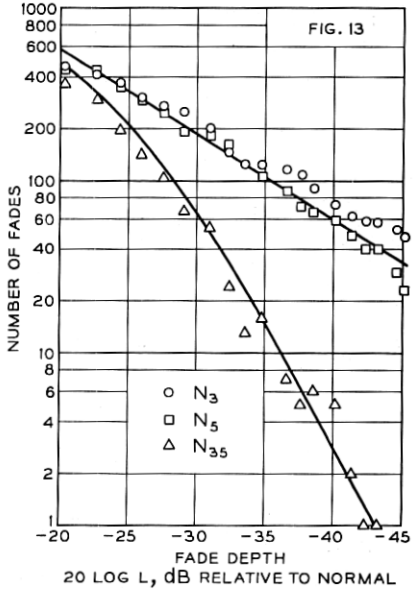

Fig. 10—Number of fades in test period (6-GHz band, $\Delta f = 60$ MHz).
Fig. 11—Number of fades in test period (6-GHz band, $\Delta f = 60$ MHz).
Fig. 12—Number of fades in test period (6-GHz band, $\Delta f = 90$ MHz).
Fig. 13—Number of fades in test period (6-GHz band, $\Delta f = 90$ MHz).

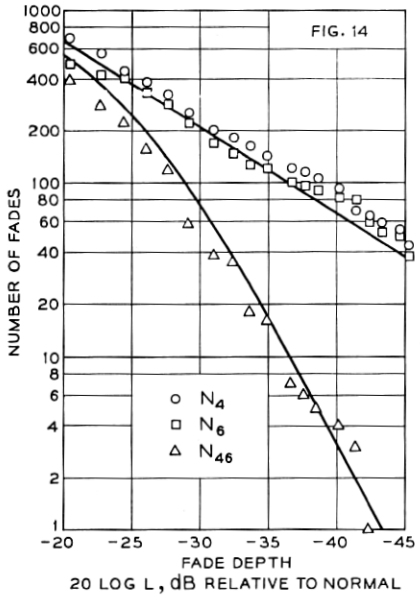

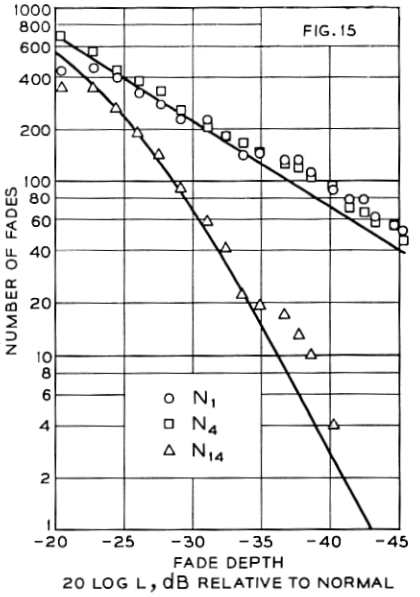

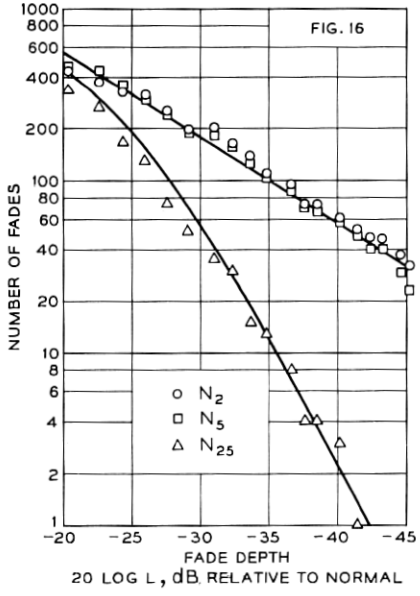

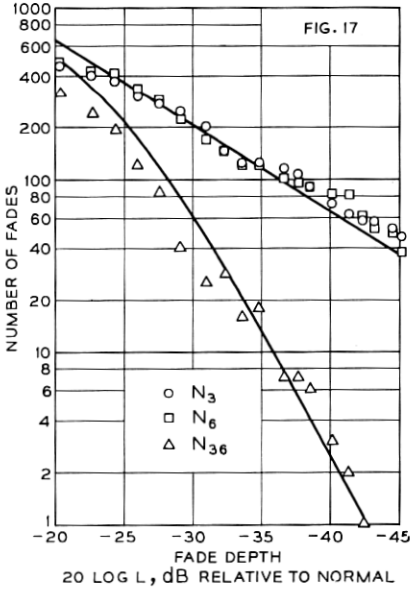

Fig. 14—Number of fades in test period (6-GHz band, $\Delta f = 90$ MHz).
Fig. 15—Number of fades in test period (6-GHz band, $\Delta f = 120$ MHz).
Fig. 16—Number of fades in test period (6-GHz band, $\Delta f = 120$ MHz).
Fig. 17—Number of fades in test period (6-GHz band, $\Delta f = 120$ MHz).

for the 6-GHz band and Figs. 21 to 35 for the 4-GHz band. The figures are arranged in order of increasing frequency separation in each of the two bands. The number of fades of R_i in the test period is denoted by N_i. The number of simultaneous fades in the test period is denoted by N_{ij}. The points on the drawings are the experimental data; the lines are theoretical and will be discussed shortly.

The data show, for example, that for a one percent frequency separation in the 6-GHz band (60 MHz, Figs. 9 to 11) N_{ij} averages to about one -40 dB fade per ten days. The ratio of N_i to N_{ij} at this fade depth is about ten.

The number of deep simultaneous fades is roughly proportional to L^3, which again suggests comparison to theoretical results for Rayleigh distributed variables. When R_i and R_j are treated as correlated Rayleigh distributed variables, the theoretical expression for the number of deep simultaneous fades is[9]

$$N_{ij} \approx (rT_0c)2q^{-1}L^3, \quad L < 0.1, \quad q^{-1}L^2 < 0.1 \tag{8}$$

where the parameter q is a function of the frequency separation of the signals. Values of q for the various signal pairs are listed in Tables II and III.*

The comparison of the theoretical expressions to the experimental data was carried out as follows. Values of q for the various signal pairs (R_i, R_j) were obtained from Table II or Table III. On each drawing, equation (6) was used to describe the average of N_i and N_j, and equation (8) was used to describe N_{ij}. Actually, equation (8) describes only the part of N_{ij} appearing as a straight line on a drawing; the curved portions of N_{ij} were computed from more complex expressions in previous work.[9] The value of q determines the position of equation (8) relative to equation (6), and curve fitting becomes a matter of fitting two curves with a fixed relative position to the three sets of data on a drawing. The result of a fitting is a value for the product rT_0c. The values of rT_0c vary somewhat from drawing to drawing, reflecting the apparently random variations in N_i from signal to signal. The average values of rT_0c in the two frequency bands appear as coefficients in equations (2) and (3). The overall impression is that the data agree with the theoretically predicted dependence on the fade depth L.

The behavior of the data on the number of fades is typically that of

* These are values of q obtained by Barnett[2] for each signal pair from experimental data on fade depth distributions. Equations describing q are shown in Section X.

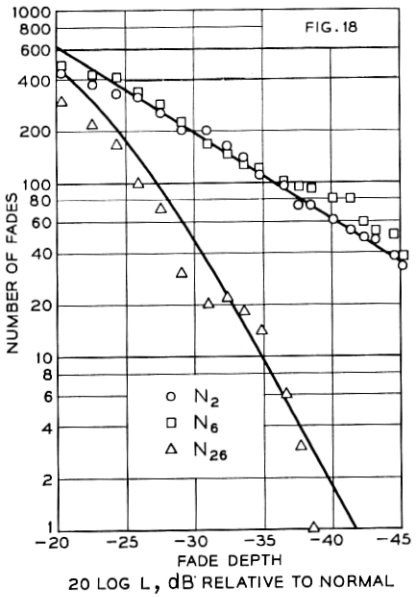

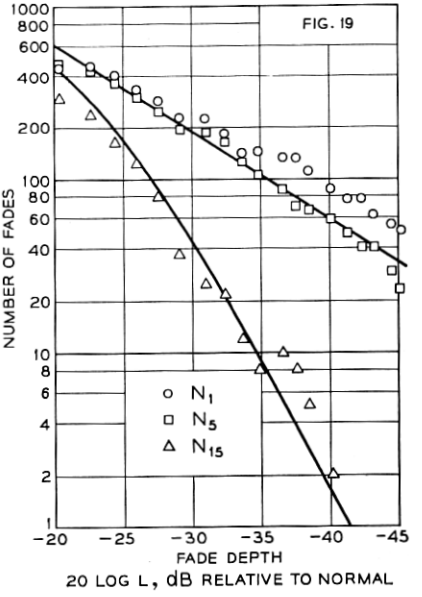

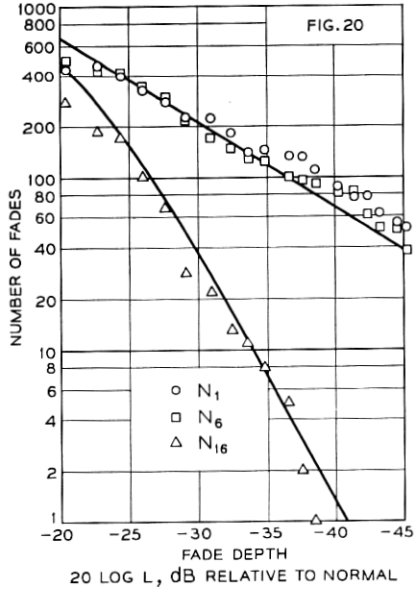

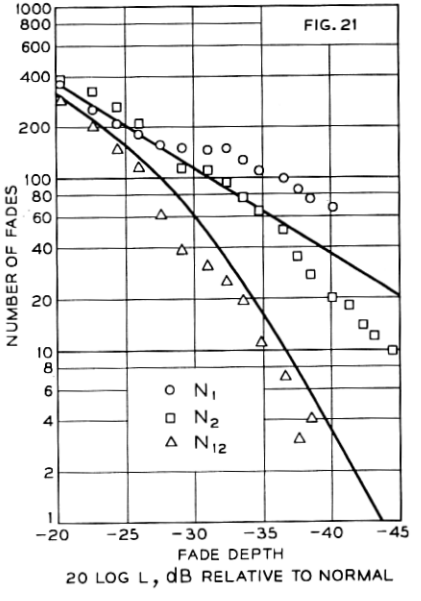

Fig. 18—Number of fades in test period (6-GHz band, $\Delta f = 150$ MHz).
Fig. 19—Number of fades in test period (6-GHz band, $\Delta f = 180$ MHz).
Fig. 20—Number of fades in test period (6-GHz band, $\Delta f = 210$ MHz).
Fig. 21—Number of fades in test period (4-GHz band, $\Delta f = 20$ MHz).

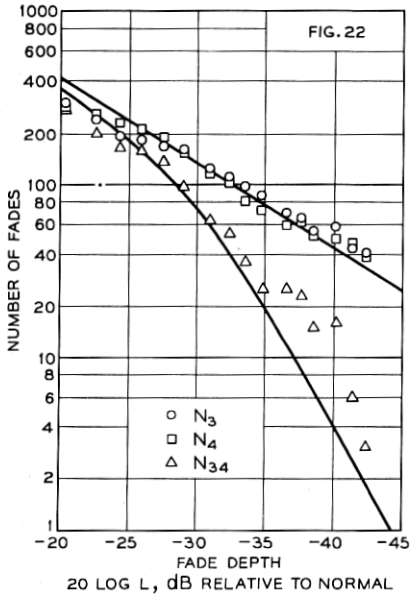

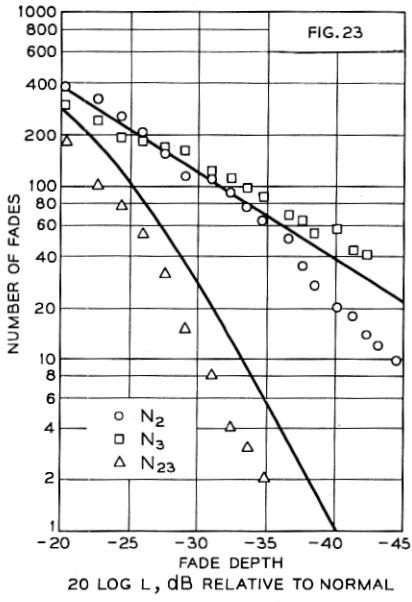

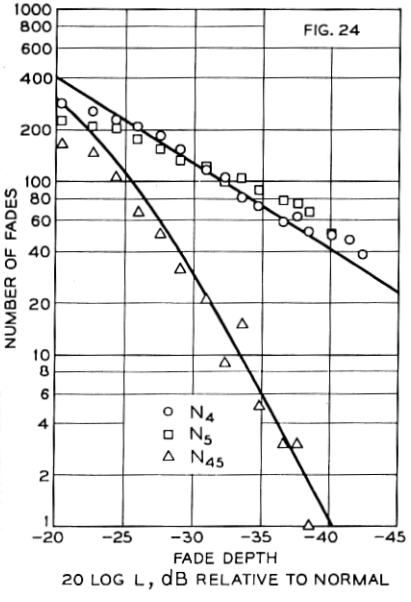

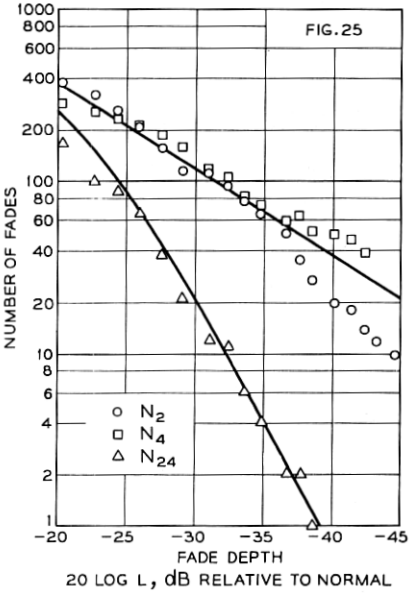

Fig. 22—Number of fades in test period (4-GHz band, $\Delta f = 20$ MHz).
Fig. 23—Number of fades in test period (4-GHz band, $\Delta f = 60$ MHz).
Fig. 24—Number of fades in test period (4-GHz band, $\Delta f = 60$ MHz).
Fig. 25—Number of fades in test period (4-GHz band, $\Delta f = 80$ MHz).

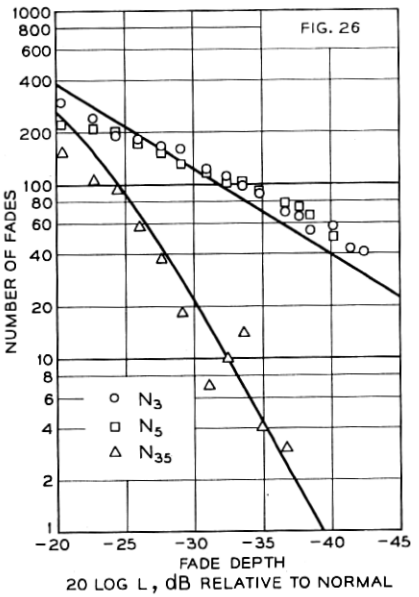

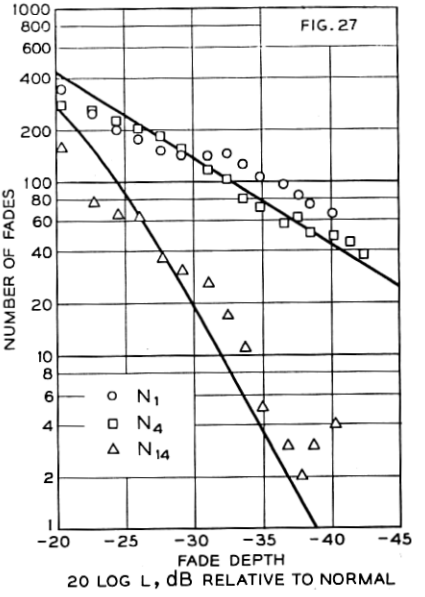

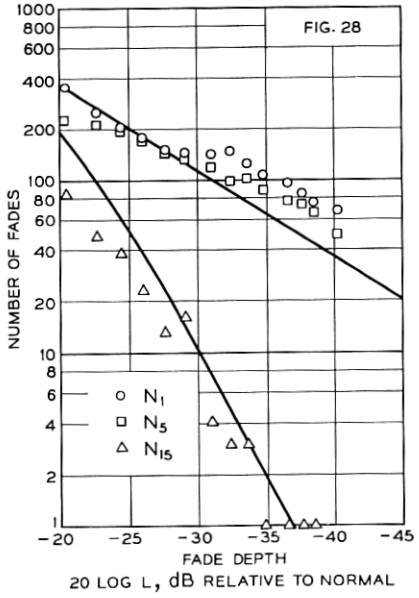

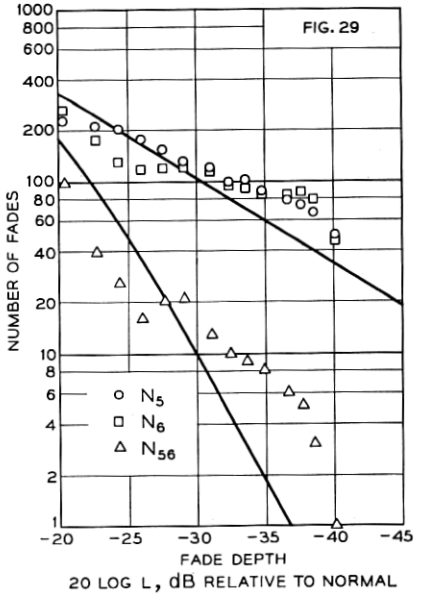

Fig. 26—Number of fades in test period (4-GHz band, $\Delta f = 80$ MHz).
Fig. 27—Number of fades in test period (4-GHz band, $\Delta f = 100$ MHz).
Fig. 28—Number of fades in test period (4-GHz band, $\Delta f = 160$ MHz).
Fig. 29—Number of fades in test period (4-GHz band, $\Delta f = 160$ MHz).

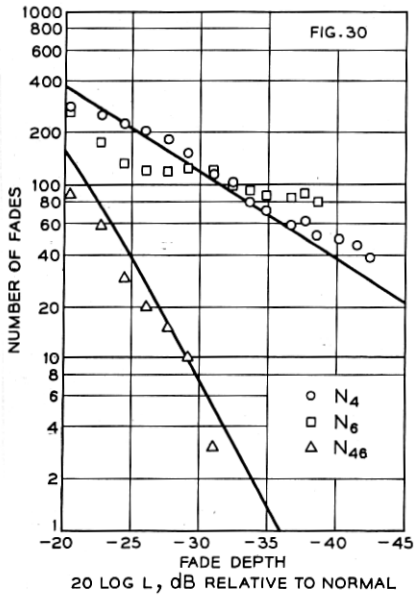

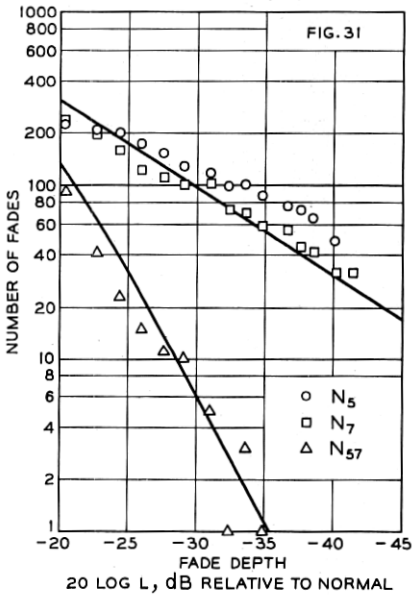

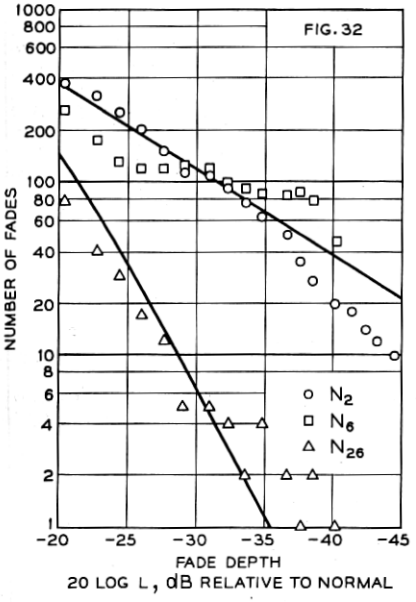

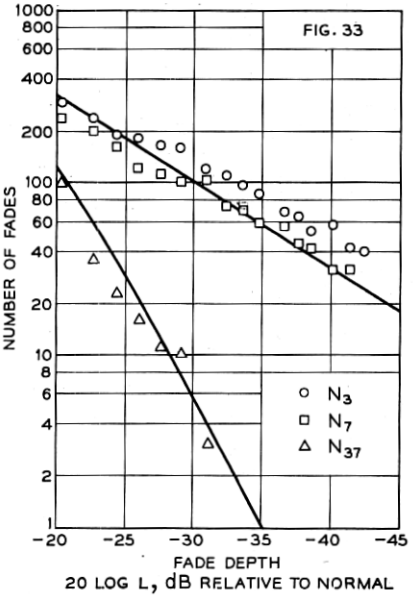

Fig. 30—Number of fades in test period (4-GHz band, $\Delta f = 220$ MHz).
Fig. 31—Number of fades in test period (4-GHz band, $\Delta f = 260$ MHz).
Fig. 32—Number of fades in test period (4-GHz band, $\Delta f = 300$ MHz).
Fig. 33—Number of fades in test period (4-GHz band, $\Delta f = 340$ MHz).

propagation data in general. The processes in the atmosphere causing fading are complex, and this shows up as scatter and deviations of the experimental points from the theoretical lines. Some of this is magnified by the logarithmic scales used in the drawings. The deviations of the experimental points from the theoretical lines in the 4-GHz band are larger than those in the 6-GHz. This may be because the number of observations in the 4-GHz band is smaller, or because the theoretical description becomes less applicable as the path length, measured in wavelengths, becomes shorter. The deviations of the points from the lines around −20 dB reinforce the observation that the theory based on the joint Rayleigh distribution applies only to fades deeper than about −20 dB. A possible explanation is that the physical processes generating deep fades differ from those generating shallow fades.

V. AVERAGE DURATION OF SIMULTANEOUS FADES

The determination of the average durations of simultaneous fades is difficult, because there are too few simultaneous fades, particularly at the larger frequency separations, to obtain meaningful averages. The data for the first entry in Table II are shown in Fig. 36. The curves are theoretical. The top curve is equation (7), with c^{-1} adjusted to describe the average of α_2 and α_3 (the notation is defined in Fig. 1). Given the top curve and the value of q in Table II, the bottom curve describing β_{23} is calculated under the assumption that R_2 and R_3 are jointly Rayleigh distributed.[9] Note from the curves that as the fades become deeper, the average durations of simultaneous fades tend to one-half of those of single signals. The theory predicts this for all frequency separations, provided the fades are sufficiently deep,[9]

$$\langle \beta_{ij} \rangle \approx \tfrac{1}{2}\langle \alpha_i \rangle, \quad L < 0.1, \quad q^{-1}L^2 < 0.1. \tag{9}$$

It is interesting that the same result can also be inferred from a heuristic argument, given in Section VIII.

The data and the theory are in agreement in Fig. 36. In general, the data on the average durations of simultaneous fades show a large amount of scatter, much larger than in the example in Fig. 36, because of the small number of observations.

VI. THE SCALE OF SCATTER IN THE OBSERVATIONS

Experimental data can scatter simply because the number of observations is small. In the case of average fade durations we can esti-

mate the amount of scatter possible, and it is instructive to digress and do so. As an example, the average durations at the highest frequency in the 6-GHz band are shown in Fig. 37 (the points denoted by black squares are at fade depths for which probability distributions of fade durations will be obtained later). Each point on the drawing is the average of a sample of size N_i. This average, the so called sample mean, is a random variable. For example, if the test period contains, by chance, an excess of small α_i, the sample mean will be less than the true average. As N_i increases, the sample mean tends to deviate less from the true average. The standard deviations of the sample means in Fig. 37 are estimated in the Appendix. The straight line in Fig. 37 is the result of a least squares fitting of equation (7) to the data. The curves are at three standard deviations of the sample mean above and below the straight line.

The tolerance band defined by the curves in Fig. 37 is asymmetric, especially so for the deeper fades, because of the logarithmic scale on which the average fade durations are plotted. The band is quite wide in the -40 dB region, and the conclusion is that the deviations of the points from the line are well within those predicted possible by elementary sampling theory.

A corresponding tolerance band for the 4-GHz data would be wider because of the smaller number of fades observed. It would be much wider for the simultaneous fades because their number is much smaller. Because of the potential for large scatter in the 4-GHz data, we will discuss, in the next section, duration distributions for the 6-GHz band only.

VII. OBSERVED DISTRIBUTIONS OF FADE DURATIONS

Estimates of the probability that a fade of depth 20 log L dB (see Fig. 1) lasts longer than t seconds were obtained by taking the number of fades longer than t seconds and dividing this by the total number of fades of depth 20 log L dB. The results of this for the highest frequency in the 6-GHz band are shown in Fig. 38 for five values of fade depth (the average durations at these depths are denoted by the black squares in Fig. 37). The probability scale is normal and the duration scale is logarithmic.

The behavior of the probabilities shows a more readily discernible pattern if the durations are measured not in seconds but in units of average fade durations; that is, if we look at the probability that x_i is larger than a number u, where

$$x_i = \alpha_i / \langle \alpha_i \rangle. \tag{10}$$

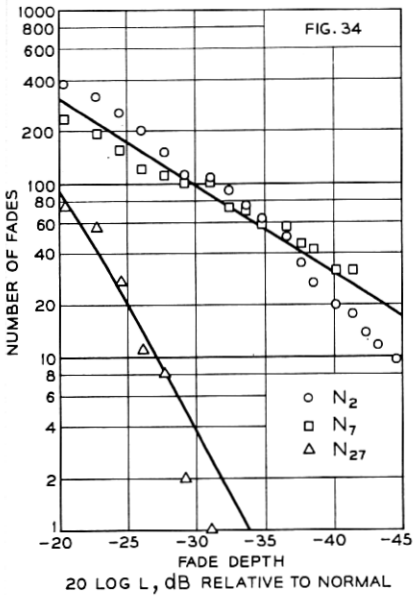

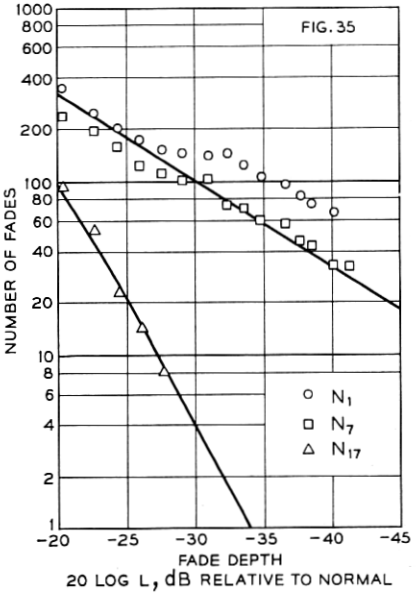

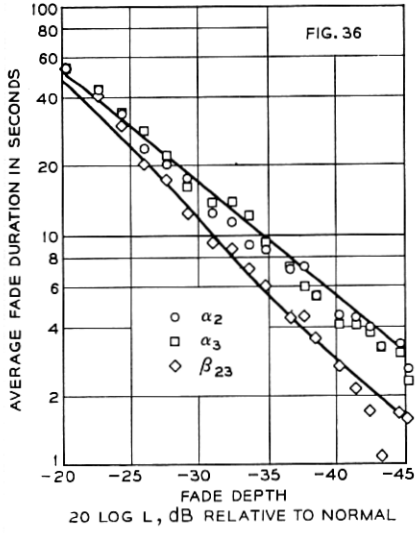

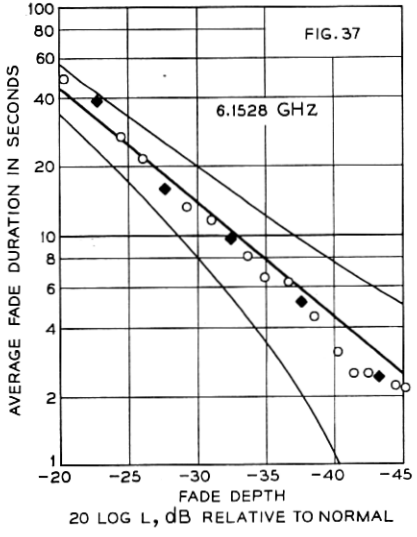

Fig. 34—Number of fades in test period (4-GHz band, $\Delta f = 400$ MHz).
Fig. 35—Number of fades in test period (4-GHz band, $\Delta f = 420$ MHz).
Fig. 36—Average durations of simultaneous fades of signals at 6.0045 and 6.0342 GHz (the lines are theoretical)
Fig. 37—Average durations of fades of the signal at 6.1528 GHz, with superimposed control curves at three standard deviations above and below the straight line, estimated from elementary sampling theory.

When this is done, using values of $\langle \alpha_i \rangle$ denoted by solid squares in Fig. 37, the fairly tightly grouped set of points in Fig. 39 is obtained. From the behavior of the points for the various fade depths one can argue that the data approach a lognormal distribution, denoted by the straight line, as fades become deeper and longer. When points from the other five frequencies are superimposed on this, Fig. 40 is obtained. Because we have pooled data from various frequencies, we have dropped the subscripts on the variables.

The pattern formed by the points in Fig. 40 suggests that the distribution of durations longer than average can be described by a straight line (the points for the long durations begin to scatter because the number of observations is small). The equation of the line shown is

$$\Pr(x > u) = \tfrac{1}{2} \operatorname{erfc} [(\ln u - \mu)/\sqrt{2}\,\sigma] \tag{11}$$

with

$$\mu = -0.673, \quad \sigma = 1.27 \tag{12}$$

where ln denotes the natural logarithm, and erfc denotes the complementary error function. The lognormal distribution (11) specifies that one percent of the durations are longer than ten times average, and that thirty percent of the durations are longer than average.

The results for the durations of the simultaneous fades also fall into a pattern when the durations are normalized to their averages. Letting

$$y_{ij} = \beta_{ij}/\langle \beta_{ij} \rangle \tag{13}$$

and pooling the data for all fifteen entries in Table II, we obtain Fig. 41. Again, subscripts are dropped for the pooled data.

The behavior of the data for the simultaneous fades in Fig. 41 is very similar to that of the data in Fig. 40. The line from Fig. 40 is shown dotted on Fig. 41 (the solid line on Fig. 41 will be discussed shortly).

Comparison to previous data on duration distributions[5-7] is difficult, beyond noting the similar lognormal behavior, since the previous data do not cover fades in the -30 to -40 dB range of interest to us. Furthermore, in one of the cases the emphasis is on a grazing path[5, 6] and in the other on overwater paths,[7] whereas our interest is in "standard" overland paths.

VIII. THEORETICAL DESCRIPTION OF DURATION DISTRIBUTIONS

The probability distribution of α_i is related to the power spectrum of the fluctuations of R_i.[11] Calculation of the probability distribution of

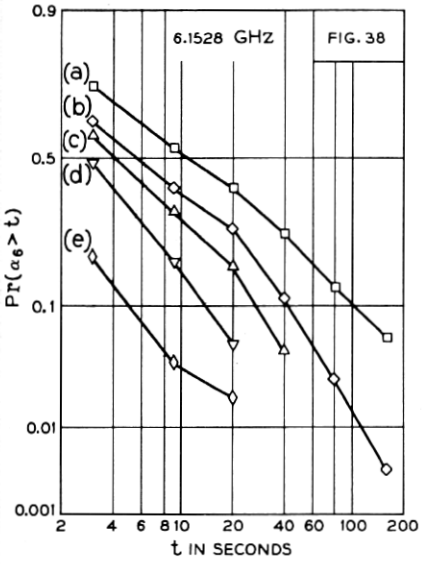

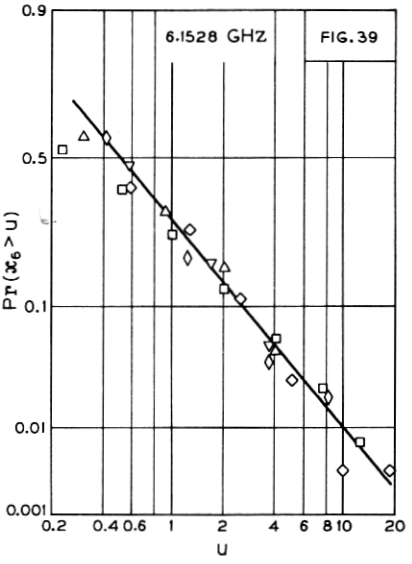

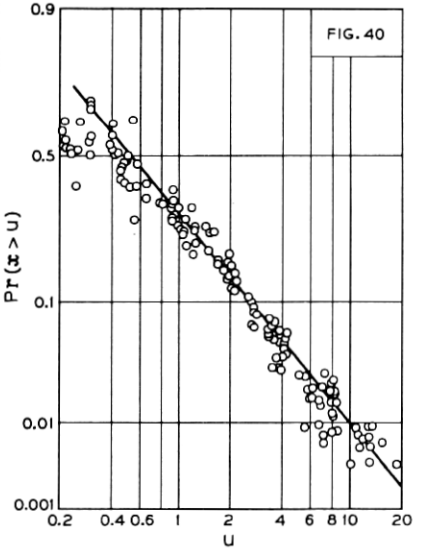

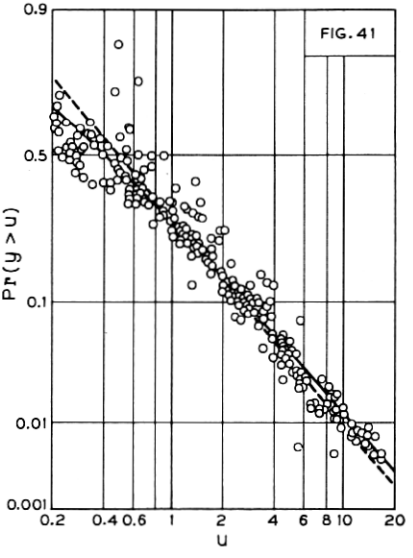

Fig. 38—Probability that duration of fade is longer than a given number of seconds for five fade depths [20 log L is: (a) −22.7 dB, (b) −27.6 dB, (c) −32.4 dB, (d) −37.6 dB, (e) −43.2 dB].

Fig. 39—Probability that duration of fade, normalized to its mean, is longer than a given number (same data as on Fig. 38—line fitted to show trend for deep fades).

Fig. 40—Probability that duration of fade, normalized to its mean, is longer than a given number (summary for the six signals in the 6-GHz band at the fade depths listed for Fig. 38—the line is from Fig. 39).

Fig. 41—Probability that duration of a simultaneous fade, normalized to its mean, is longer than a given number (summary for the 15 pairs of signals in the 6-GHz band listed in Table II—dotted line from Fig. 39—solid line is theoretical).

α_i is difficult theoretically and also because we do not have experimental information on the power spectra. Experimental determination of the spectra is far from straightforward, because fading occurs in spurts and because, presumably, the fluctuations of R_i are generated by a mix of random processes. Various theoretical spectra have been treated by S. O. Rice[11] (we obtained the idea of normalizing to the average durations from this work), but our observed durations are longer than those that follow from the spectra considered. For example, the spectrum that gives the largest percentage of long durations provides one percent of durations longer than 5.6 times the average (from Fig. 4 in Ref. 11). The data in Fig. 40 show that one percent of the durations are longer than ten times average.

To circumvent these difficulties we use the empirically determined expression (11) for $\Pr(x > u)$, and determine the duration distribution of simultaneous fades from this using a heuristic model. The model is based on the observation that when signals separated in frequency undergo a deep fade, the fade durations are often roughly the same, but the fades are offset in time. Furthermore, as fades become deeper they become shorter, and the offsets soon become larger than the fade durations, which explains why there is a large reduction in the number of deep simultaneous fades. A simultaneous fade occurs when the fades at two frequencies overlap. There is apparently no preferred overlap position, and the relationship between α and β (see Fig. 1) can be expressed mathematically as

$$\beta = g\alpha \tag{14}$$

where g is a random variable, distributed uniformly between zero and unity. The relationship (9) for the averages follows from this immediately.

The duration distribution of the simultaneous fades also follows immediately when the transformation (14) is applied to $\Pr(x > u)$. Specifically,

$$\begin{aligned} \Pr(y > u) &= \Pr(2gx > u), \\ &= \int_0^1 \Pr(x > \tfrac{1}{2}g^{-1}u)\, dg, \end{aligned} \tag{15}$$

where the integrand is (11), with appropriate change of variable. Fortunately, this can be transformed into an expression that can be integrated.[13] The result, after a fair amount of algebra, is

$$\Pr(y > u) = \tfrac{1}{2}\operatorname{erfc}\left(\frac{\ln(\tfrac{1}{2}u) - \mu}{\sqrt{2}\,\sigma}\right)$$

$$- \tfrac{1}{4}u \exp(-\mu + \tfrac{1}{2}\sigma^2)\operatorname{erfc}\left(\frac{\ln(\tfrac{1}{2}u) - \mu}{\sqrt{2}\,\sigma} + \frac{\sigma}{\sqrt{2}}\right). \quad (16)$$

The solid line in Fig. 41 is equation (16) with numerical values for μ and σ as in equation (12). The line provides adequate description of durations longer than average.

The generality imparted to the distribution functions $\Pr(x > u)$ and $\Pr(y > u)$ by the normalization of the durations to their means is a subject for further work. We would venture a guess, for example, that the distributions of x and y in the 4-GHz band are also given by equations (11) and (16). A somewhat different thought is that the idea of uniformly distributed overlaps of deep fades, which lead to equation (14), can perhaps be extended to durations of simultaneous fades of more than two signals. This approach might provide results for a problem that otherwise seems to be mathematically intractable.

IX. SIMILARITY TO DURATION DISTRIBUTION IN BEYOND-HORIZON PROPAGATION

It is interesting to compare the line-of-sight data for $\Pr(x > u)$ to similar data for tropospheric beyond-horizon propagation,[14] where fade durations have also been observed to be lognormally distributed. Table IV shows that the numerical values for line-of-sight (from our Fig. 40) are quite close to the numerical values for long term tropospheric data (from Table 2 of Ref. 14).

In line-of-sight transmission, the receiving antenna is illuminated directly by the transmitting antenna. In beyond-horizon tropospheric transmission the receiving antenna is illuminated by reflected (scattered) energy. There is insufficient knowledge to decide whether the

TABLE IV—COMPARISON OF FADE-DURATION PROBABILITIES IN LINE-OF-SIGHT AND BEYOND-HORIZON PROPAGATION

	u	
$\Pr(x > u)$	Line-of-Sight	Beyond-Horizon
0.1	2.6	2.2
0.01	10	9.1

structures of the electromagnetic waves at the receiving antennas in the two cases are similar in some sense, or whether the numerical closeness of the distributions of the durations normalized to their means is accidental.

X. COMPARISON OF FREQUENCY AND SPACE DIVERSITY

The number of simultaneous fades of the two signals must be small to obtain good diversity reception. More specifically, the ratio

$$F_N = N_i/N_{ij} \tag{17}$$

must be large. For signal envelopes that are jointly Rayleigh distributed, a theoretical result for deep fades is[9]

$$F_N \approx \tfrac{1}{2}qL^{-2}, \quad L < 0.1, \quad q^{-1}L^2 < 0.1. \tag{18}$$

This shows how F_N varies with fade depth. Information about the separation of the signals is contained in the parameter q. A theory from which q can be calculated for line-of-sight microwave links still remains to be established. However, empirical expressions for q, based on experimental data, are available,[2] and these provide a means for comparing the effectiveness of separations in frequency and space.

For separations in frequency, expressions for q determined from probability distributions of R_{ij} are[2]

$$q = \tfrac{1}{4}(\Delta f/f), \text{ in the 6-GHz band;} \tag{19}$$

$$q = \tfrac{1}{2}(\Delta f/f), \text{ in the 4-GHz band;} \tag{20}$$

where Δf is the frequency separation of R_i and R_j, and where the values of f used in the determination of the coefficients in equations (19) and (20) were 6.175 and 3.950 GHz respectively. The above expressions for q are based on data obtained on a 28.5-mile path in Ohio. We do not know, for example, how the expressions are affected by changes in path length.

For two signals received at the same frequency on two vertically separated receiving antennas, an empirical expression for q is[8, 9]

$$q = (2.75)^{-1}(s^2/\lambda d) \tag{21}$$

where s is the vertical center-to-center separation of the receiving antennas, λ is the wavelength, and d is the path length—all measured in the same units. Equation (21) is also based on data from the test path in Ohio, which was picked because fading on it was thought to be typical of many paths in the United States. Some generality is lent

to equation (21) by the fact that one of the experimental points on which it is based comes from data obtained in Texas.

The equations for q can be used to compare the effects of separations in frequency and space. For example, separations that provide equal values of F_N are shown in Fig. 42. The curves apply for deep fades that satisfy the conditions $L < 0.1$ and $q^{-1}L^2 < 0.1$. As an illustration, values of F_N at 20 log $L = -40$ are indicated along the curves. Since the expressions for q are based on data for fairly small separations, equations (19) through (21) should be viewed as first terms in power series, and extrapolation of the results to separations larger than those in Fig. 42 may not be advisable.

The term improvement has been used to describe the ratio of the total time spent in fades to the total time spent in simultaneous fades.[2, 8] In terms of F_N, the deep fade approximation for the improvement F is[9]

$$F \approx 2F_N, \quad L < 0.1, \quad q^{-1}L^2 < 0.1 \tag{22}$$

and Fig. 42 therefore describes separations that provide equal improvement.

XI. CONCLUSIONS

We have presented data on aspects of fading that are important but have not been covered in previous investigations of fading on line-of-

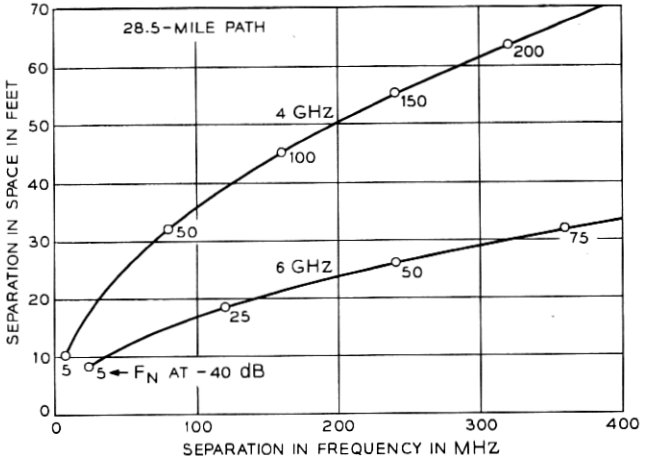

Fig. 42—Separations in space and in frequency that provide equal values of the ratio of the number of fades to the number of simultaneous fades.

sight microwave links. The theoretical framework we have provided for the data will be, we anticipate, of practical value to designers of communication systems.

The results presented here also demonstrate that further work, both experimental and theoretical, is needed. For example, the parameters in our equations are empirical and are based on data from one propagation path only.

XII. ACKNOWLEDGMENTS

The data presented come from an experiment to which many people at Bell Laboratories have contributed. From an overall point of view, there are three equally important parts to the work associated with the experiment. First, the design of the Multiple Input Data Acquisition System (MIDAS) by G. A. Zimmerman. Second, data processing, based on the work and ideas of C. H. Menzel. Third, data analysis and theory, which is our own area of work. In all parts of the work, discussions with W. T. Barnett have been invaluable.

APPENDIX

Control Curves

The equation for the control curves in Fig. 37 is, denoting the standard deviation of the sample means by σ_s,

$$f(L) = \langle \alpha_i \rangle \pm 3\sigma_s . \tag{23}$$

From elementary sampling theory[15]

$$\sigma_s^2 = N_i^{-1}\sigma_\alpha^2 \tag{24}$$

where σ_α is the standard deviation of the fade durations α_i. Further

$$\sigma_\alpha = \langle \alpha_i \rangle \sigma_x \tag{25}$$

where σ_x is the standard deviation of x, and x denotes the fade durations normalized to their means. The probability distribution of the natural logarithm of x is given by equation (11). In terms of the variance of that distribution

$$\sigma_x^2 = \langle x \rangle^2 (\exp(\sigma^2) - 1). \tag{26}$$

Since $\langle x \rangle$ is unity by definition, use of σ from equation (12) gives

$$\sigma_x^2 \approx 4. \tag{27}$$

Using equation (2) to describe N_i, we obtain

$$f(L) \approx \langle \alpha_i \rangle \left\{ 1 \pm \frac{6}{\sqrt{6410L}} \right\}. \tag{28}$$

The straight line in Fig. 37 is $\langle \alpha_i \rangle$, and equation (28) therefore provides numerical values for drawing of the control curves.

REFERENCES

1. Kaylor, R. L., "A Statistical Study of Selective Fading of Super-High Frequency Radio Signals," B.S.T.J., *32*, No. 5 (September 1953), pp. 1187–1202.
2. Barnett, W. T., "Microwave Line-of-Sight Propagation with and without Frequency Diversity," B.S.T.J., *49*, No. 8 (October 1970), pp. 1827–1871.
3. Baker, A. E., and Brice, P. J., "Radio-Wave Propagation as a Factor in the Design of Microwave Relay Links," Post Office Elec. Eng. J., *62*, No. 4 (January 1970), pp. 239–246.
4. Ugai, S., "Characteristics of Fading due to Ducts and Quantitative Estimation of Fading," Rev. Elec. Commun. Lab. (Japan), *9*, No. 5–6 (May–June 1961), pp. 319–360.
5. Wheeler, B. F., and Mathwich, H. R., "Use of Distribution Curves in Evaluating Microwave Path Clearance," IRE Trans. Instrumentation, *PGI-4*, (October 1955), p. 31.
6. Mathwich, H. R., Nuttall, E. D., Pitman, J. E., and Randolph, A. M. "Propagation Test on 955.5 Mc, 1965 Mc and 6730 Mc," AIEE Trans. Commun. Elec., Part I, *75* (January 1957), pp. 685–691.
7. Gudmandsen, P., and Larsen, B. F., "Statistical Data for Microwave Propagation Measurements on Two Oversea Paths in Denmark," Trans. IRE on Antennas and Propagation, *AP-5*, No. 3 (July 1957), pp. 255–259.
8. Vigants, A., "Space-Diversity Performance as a Function of Antenna Separation," IEEE Trans. Commun. Tech., *COM-16*, No. 6 (December 1968), pp. 831–836.
9. Vigants, A., "The Number of Fades in Space-Diversity Reception," B.S.T.J., *49*, No. 7 (September 1970), pp. 1513–1530.
10. Pearson, K. W., "Method for the Prediction of the Fading Performance of a Multisection Microwave Link," Proc. IEE (London), *112*, No. 7 (July 1965), pp. 1291–1300.
11. Rice, S. O., "Distribution of the Duration of Fades in Radio Transmission: Gaussian Noise Model," B.S.T.J., *37*, No. 3 (May 1958), pp. 581–635.
12. Barnett, W. T., "Occurrence of Selective Fading as a Function of Path Length, Frequency, and Geography," 1969 USNC/URSI Spring Meeting, April 21–24, 1969, Washington, D. C.
13. Abramowitz, M., and Stegun, I. A., editors, *Handbook of Mathematical Functions*, New York: Dover Publications, 1965, p. 304.
14. Grosskopf, J., and Fehlhaber, L., "Rate and Duration of Single Deep Fades in Tropospheric Scatter Links," NTZ-Commun. J., *1*, No. 3 (1962), pp. 125–132.
15. Hoel, P. G., *Introduction to Mathematical Statistics*, New York: John Wiley & Sons, 1954, pp. 105–109.